

$^{87}\text{Y}(n,\gamma)$ and $^{89,90}\text{Zr}(n,\gamma)$ cross sections from a surrogate reaction approach

Shuya Ota^{1,a}, J.T. Burke¹, R.J. Casperson¹, J.E. Escher¹, R.O. Hughes¹, J.J. Ressler¹, N.D. Scielzo¹, I. Thompson¹, R.A.E. Austin², E. McCleskey³, M. McCleskey³, A. Saastamoinen³, T. Ross⁴

¹Lawrence Livermore National Laboratory, Livermore, CA, 94551 USA

²Saint Mary's University, Halifax, Nova Scotia, Canada

³Cyclotron Institute, Texas A&M University, College Station, TX, USA

⁴Department of Chemistry, University of Kentucky, Lexington, KY, USA

Abstract. The surrogate reaction approach is an indirect method for determining nuclear reaction cross sections which cannot be measured directly or predicted reliably. While recent studies demonstrated the validity of the surrogate reaction approach for studying fission cross sections for short-lived actinides, its applicability for radiative neutron capture reactions ((n,γ)) is still under investigation. We studied the γ decay of excited ^{88}Y and $^{90,91}\text{Zr}$ nuclei produced by $^{89}\text{Y}(p,d)$, $^{91}\text{Zr}(p,d)$, and $^{92}\text{Zr}(p,d)$ reactions, respectively, in order to infer the $^{87}\text{Y}(n,\gamma)$ and $^{89,90}\text{Zr}(n,\gamma)$ cross sections. The experiments were carried out at the K150 Cyclotron facility at Texas A&M University with a 28.5-MeV proton beam. The reaction deuterons were measured at forward angles of 25–60° with the array of three segmented Micron S2 silicon detectors. The compound nuclei with energies up to a few MeV above the neutron separation thresholds were populated. The coincident γ -rays were measured with the array of five Compton-suppressed HPGe clover detectors.

1 Introduction

While radiative neutron capture reaction ((n,γ)) cross sections of short-lived isotopes at energies from several keV to tens of MeV play important roles in nuclear physics topics such as nuclear astrophysics [e.g., 1, 2], nuclear energy [3], and radiochemical applications [4], the cross sections remain unknown for most isotopes because of their inaccessibility as target materials. Even with the development of radioactive ion beam facilities, the (n,γ) cross sections cannot be measured using inverse-kinematics because a neutron target does not exist. Theoretical prediction of the cross sections can be unreliable when detailed nuclear structure information is unavailable. Thus, the development of indirect methods to determine the cross sections is required. Here, the present status in the study of the surrogate reaction approach to infer the (n,γ) cross sections for the mass region of Zr/Y ($A\sim 90$) is described.

Although the surrogate reaction approach was developed for measurements of neutron-induced fission ((n,f)) cross sections of actinides in 1970's [5, 6], it has attracted a renewed attention in the past decade due to interest in minor actinides from nuclear reactor physics and stockpile stewardship [7]. While the applicability of the surrogate reaction approach has been demonstrated for (n,f) cross sections [8–12], it has been difficult to

determine (n,γ) cross sections due primarily to the discrepancy in the spin-parity distributions of the compound nucleus created by the (n,γ) and the surrogate reaction [13–17]. However, some recent research showed promise for inferring (n,γ) cross sections by accounting for spin-parity distribution of the compound nucleus [18]. One goal of the present work is to test the validity of the approach for Y-Zr nuclei which are more spherical and therefore more sensitive to differences in the spin-parity distributions because of their lower level densities compared to minor actinides and rare-earth nuclei [7, 17].

The $^{87}\text{Y}(n,\gamma)$ and $^{89}\text{Zr}(n,\gamma)$ cross sections are very important e.g., for stockpile stewardship. However, there are no data available for these cross sections due to their short half-lives (3.35 and 3.27 days, respectively). $^{87,88}\text{Y}$ have some long-lived isomeric states (see Fig. 1) which are of interest as well. For the $^{87}\text{Y}(n,\gamma)$ measurements, the $^{89}\text{Y}(p,d\gamma)$ reaction was selected as the best way to access ^{88}Y compound nucleus since ^{89}Y is the only stable yttrium isotope. On the other hand, in case of $^{89}\text{Zr}(n,\gamma)$, there are many stable isotopes such as $^{90,91,92,94,96}\text{Zr}$, for which directly-measured (n,γ) cross sections data already exist. Thus we can use $^{91}\text{Zr}(p,d\gamma)$ reaction to determine $^{89}\text{Zr}(n,\gamma)$, and the $^{92}\text{Zr}(p,d\gamma)$ reaction to determine the known $^{90}\text{Zr}(n,\gamma)$ cross section to benchmark the approach.

^a Corresponding author: ota2@llnl.gov

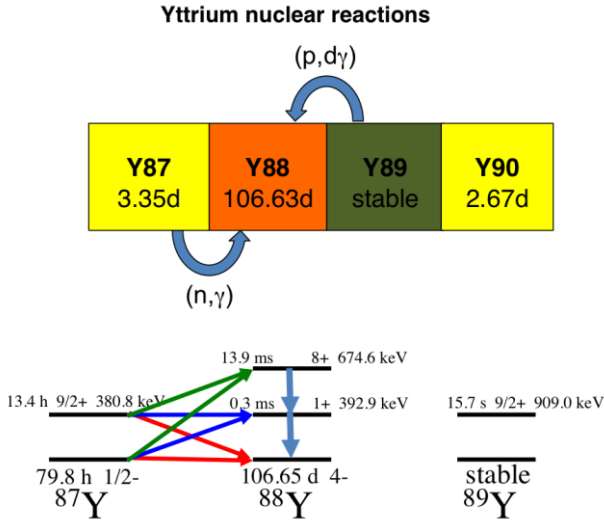


Figure 1. (Upper panel) Half lives of Y isotopes. (Lower panel) Isomeric states of $^{87,88,89}\text{Y}$.

2 Surrogate reaction approach for (n,γ)

A detailed description of the surrogate reaction approach is presented in Ref. [7]. Here, we briefly explain the principle of the surrogate reaction approach with a focus on (n,γ) measurements.

The basic concept in the surrogate approach is the Bohr compound-nucleus hypothesis which assumed that the formation and decay of a compound nucleus are independent of each other. In other words, once the compound nucleus is created by a reaction, the decay does not depend on the formation process. This assumption does not take into account width-fluctuation corrections which are typically small and are not included at the moment [7]. Therefore, the (n,γ) cross sections ($\sigma_{(n,\gamma)}$) can be written as

$$\sigma_{(n,\gamma)} = \sum_{J,\pi} \sigma_{n+target}^{CN}(E,J,\pi) \cdot G_{\gamma}^{CN}(E,J,\pi), \quad (1)$$

where $\sigma_{n+target}^{CN}$ is the compound nucleus formation cross section for the reaction of a neutron and the target nucleus, G_{γ}^{CN} are the branching ratios for the decay of the compound nucleus, and E, J, π are energy, spin, and parity of the compound nucleus, respectively. Since the $\sigma_{n+target}^{CN}$ can be precisely calculated, $\sigma_{(n,\gamma)}$ can be determined by determining G_{γ}^{CN} from a surrogate reaction.

2.1 Limit of the WE approximation

In surrogate (p,dγ) experiments, we measure the probability $P_{(p,d\gamma)}$ which is the ratio of the number of compound-nucleus decays (by γ emission) to compound-nucleus formation events. $P_{(p,d\gamma)}$ is given by the ratio $N_{d\gamma} / (\epsilon_{\gamma} N_{singles})$ and can be used to determine G_{γ}^{CN} . Here, $N_{d\gamma}$ and $N_{singles}$ are the numbers of d-γ coincidence events which are used to identify the compound-nucleus decay

channel of interest and deuteron singles events which is used to determine the total number of compound nuclei formed, respectively. ϵ_{γ} denotes the efficiency for identifying the γ-ray cascade branch of interest including HPGe detector and internal electron conversion efficiencies. The relationship between G_{γ}^{CN} and $P_{(p,d\gamma)}$ can be formulated as eq. (2).

$$P_{(p,d\gamma)} = \sum_{J,\pi} F_{(p,d)}^{CN}(E,J,\pi) \cdot G_{\gamma}^{CN}(E,J,\pi), \quad (2)$$

where $F_{(p,d)}^{CN}$ is the formation probability of the compound nucleus in the surrogate reaction. If we apply the Weisskopf-Ewing (WE) approximation, which assumes the G_{γ}^{CN} is independent of J^{π} , we obtain that $P_{(p,d\gamma)}$ and G_{γ}^{CN} are equal. In many previous surrogate measurements, the WE approximation was used. Those surrogate measurements gave reliable results for (n,f) cross sections but gave much less accurate results for (n,γ) cross sections [7]. Therefore, G_{γ}^{CN} must be obtained from $P_{(p,d\gamma)}$ with guidance from reaction theory.

2.2 Moving beyond the WE approximation

To move away from the Weisskopf-Ewing approximation, it is necessary to predict the spin-parity population of the compound nucleus $F_{(p,d)}^{CN}(E,J,\pi)$ using theory and to model the decay of the compound nucleus in a Hauser-Feshbach-type calculation. The $G_{\gamma}^{CN}(E,J,\pi)$ obtained from such modeling are combined with the calculated $F_{(p,d)}^{CN}(E,J,\pi)$ to yield a prediction for $P_{(p,d\gamma)}(E)$. Fitting the latter to surrogate data provides further constraints on the $G_{\gamma}^{CN}(E,J,\pi)$ which can then be employed in the calculation of the desired cross section. Therefore, our goal of the experimental work is to obtain $P_{i(p,d\gamma)}$ for as many as γ-ray transitions (i) as possible.

3 Experiments

The experiments were performed at the K150 Cyclotron facility at Texas A&M University. ^{89}Y , ^{91}Zr , ^{92}Zr targets were bombarded with a 28.56-MeV proton beam with the intensity of about 1.5 nA for about 95, 36, 84 hrs, respectively. Live times in these measurements were about 70% on average. The energy spectra and angular distribution of the produced deuterons and prompt γ-rays were measured with the Silicon Telescope Array for Reactions studies, Livermore, Texas, Richmond (STARLiTeR) detector system described in the following section. While the ^{89}Y target (with the thickness of 760 $\mu\text{g}/\text{cm}^2$) is monoisotopic, the enriched $^{91,92}\text{Zr}$ targets (1 mg/cm^2 each) contain other Zr isotopes and therefore measurements using $^{90,92,94,96}\text{Zr}$ targets were made as well in order to subtract their contributions. Similarly, data was collected using a natural C target (0.1 mg/cm^2) to estimate carbon backgrounds in the targets.

Table 1. Isotopic composition of $^{91,92}\text{Zr}$ targets.

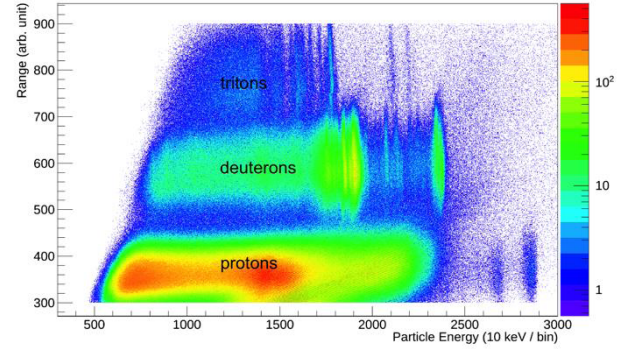
Mass number	Fraction in ^{91}Zr (%)	Fraction in ^{92}Zr (%)
90	6.51	2.86
91	88.50	1.29
92	3.21	94.57
94	1.61	1.15
96	0.17	0.14

3.1 STARLiTeR

Our detector system, STARLiTeR, is currently stationed at the K150 Cyclotron facility at Texas A&M University. STARLiTeR consists of three segmented Micron S2 silicon detectors which are segmented into 24 (maximum 48) rings and 8 (maximum 16) wedges, allowing the measurement of charged-particle scattering angles. The closest detector was at 21 mm away from the target and the array was used to identify deuterons from (p,d γ) reactions at angles between 25 and 60°. The energy resolution of STARS is typically 80 - 150 keV (FWHM). For γ -ray detection, five BGO Compton-suppressed HPGe clover detectors surrounded the silicon detector chamber are used. The total absolute photopeak efficiency is 1.5% at 500 keV and 0.5% at 2 MeV after an addback technique is applied. The energy resolution (FWHM) varies from 2 - 5 keV over the energy range of interest (0.1 - 3 MeV). Further details on the detector arrays can be found in Ref. [19]. The efficiency for γ -ray detection will be improved by increasing the number of HPGe clover detectors to 14 and the installation of this upgraded system will be completed in 2015 and help further improve accuracy of our experiments.

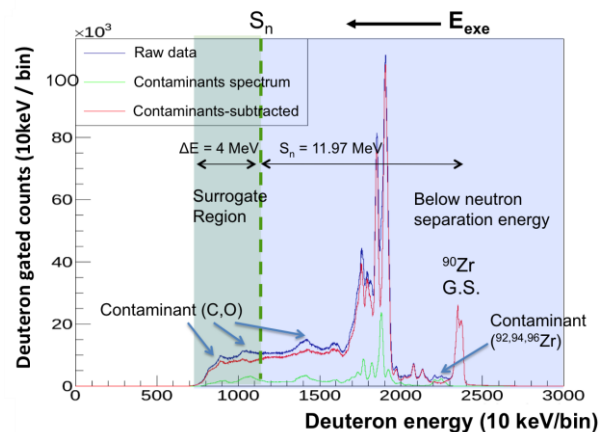
3.2 Particle Identification

A particle Identification (PID) plot from the $^{91}\text{Zr}(p,d\gamma)$ experiment is shown in Fig. 2. Unlike the conventional E- ΔE plot, we show total particle energies in the x-axis and ranges in the y-axis. The range is a quantity related to the particle range in the detector (see e.g., [13]). By the plot, a clear cut of the desired events (i.e., deuterons) was achieved. The total deuteron energies were corrected for the recoil energy of the target nuclei and energy losses in the targets and dead layers (Al and Au) of Si detectors. In Fig. 2, a deuteron peak at ~ 23.5 MeV corresponds to the ^{90}Zr ground state and the energy agrees well with a calculated value from the experimental geometry. A total of about 10^7 deuteron events were collected in the experiment.

**Figure 2.** Particle Identification from the $^{91}\text{Zr}(p,d\gamma)$ experiment.

3.3 Deuteron singles energy spectrum

Three deuteron singles spectra are shown in Fig. 3. One is taken from the runs using the ^{91}Zr target and another one is taken from the runs using $^{90,92,94,96}\text{Zr}$ and natural C targets to estimate contaminants in the ^{91}Zr target, and the last one was made from the both spectra by subtraction. The first one (blue) is the raw data spectrum without correction for any contaminants, which is a projection of the deuteron part of Fig. 2 to its x-axis. The second one (green) is the contaminants spectrum which was normalized to the experimental conditions (beam current, measurement time, live time, and so on) from the runs using ^{91}Zr target. The last one (red) is the spectrum from which contaminants are subtracted.

**Figure 3.** Deuteron singles spectrum (sum over all angles). Contaminant components are removed.

The first excited state of ^{90}Zr is 1.760 MeV above the ground state. However, some other states can be seen beyond them. These are contaminant peaks from the $^{92,94,96}\text{Zr}$ targets. Also, some peaks from the ^{12}C and ^{16}O are seen in the lower energy. These contaminant peaks are entirely removed after the correction. From the spectrum in which contaminants are removed, some more states from the ^{90}Zr are found in addition to the ground state. The 2nd excited state ($E_x = 2.186$ MeV (2^+)) is clearly seen and the mixed peaks of the 4th and the 5th excited states ($E_x = 2.739$ (4^-) and 2.747 MeV (3^-), respectively) are also clear. The 1st excited state ($E_x =$

1760 keV (0^+) is not confirmed in the figure, which support the result by Ball and Fulmer [20] who estimated the spectroscopic factor of this state is < 0.001 and the cross section is very small. The 3rd excited state ($E_x = 2.319$ MeV (5^-)) is an isomeric state, which is not found from the figure either. However, 2.319-MeV γ rays were observed in the γ -ray spectrum. Some giant peaks are found around the deuteron energies of 17-20 MeV, which are from ^{90}Zr states at $E_x=3.5$ -6.5 MeV. The neutron separation energy of ^{90}Zr is 11.97 MeV, which corresponds to ~ 11.5 -MeV deuterons. The deuteron spectrum above the threshold is used for the surrogate reaction measurement of $^{89}\text{Zr}(n,\gamma)$, which allows access to the cross section to neutron energies up to 3 - 4 MeV.

3.4 γ -ray spectrum gated by deuterons

The spectrum of γ -rays in coincidence with deuterons is shown in Figs. 4. Fig. 4 (A) and (B) show the spectrum and the correlation between energies of the deuterons and the γ -ray in the coincidence events, respectively. More than 30 peaks from the ^{90}Zr compound nucleus can be observed in the figures. Although most of them have been identified as transitions from known states, some are still under investigation.

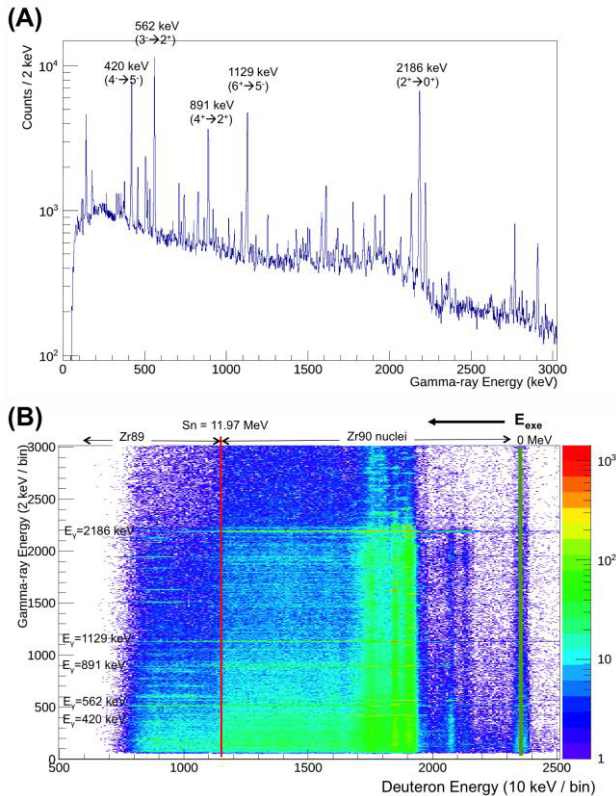


Figure 4. (A) The γ -ray spectrum gated on deuterons from the $^{91}\text{Zr}(p,d)$ experiment. (B) Correlation between the deuteron energies and the γ -ray energies in the coincidence events.

In Fig. 4 (B), it can be clearly seen that the number of events decreased suddenly above the neutron separation threshold. This is because an opening neutron emission channel suppresses the γ decay channel. To obtain the probability ($N_{d-\gamma} / N_{singles}$) for the γ -ray transitions, the number of $N_{d-\gamma}$ were measured for each peak as a function of deuteron energy. In Figs. 4, five intense peaks were indicated to demonstrate the results in the next section.

4 Results and Discussion

4.1 Probabilities

The probabilities ($P_{i(p,d\gamma)}$) for the 5 γ -ray peaks indicated in Figs. 4 are shown in Fig. 5. As expected, the probabilities start to fall above the neutron separation threshold. As discussed in Section 2, these probabilities are useful to determine the decay ratio of G^{CN}_γ . Therefore, the probabilities need to be obtained for as many peaks as possible. Currently, the probabilities for more than 30 γ peaks were collected. Data analyses of the $^{89}\text{Y}(p,d\gamma)$ and the $^{92}\text{Zr}(p,d\gamma)$ experiments are also ongoing. The inferred (n,γ) cross sections from these results will be obtained in the future.

4.2 Deuteron Angular Distributions

Angular distributions of the deuterons can be another important way to test the calculated $J\pi$ distribution of the compound nucleus. Currently, the angular distributions are being obtained for various excitation energies. Fig. 6 shows the angular distribution of deuterons from the ^{90}Zr ground state (0^+) created by the $^{91}\text{Zr}(p,d)$ experiment. The result shows a typical shape of a DWBA calculation assuming a $\Delta L = 2$ transfer which is the only possible transfer (since the ^{91}Zr ground state is $5/2^+$). This result also agrees with the work of Ball and Fulmer [20].

5 Summary

The surrogate reaction approach can be a valuable technique to access compound nucleus cross sections which cannot be measured directly and are difficult to predict reliably. The present status to constrain $^{89}\text{Zr}(n,\gamma)$ and $^{87}\text{Y}(n,\gamma)$ cross sections by the surrogate reaction approach is shown. The probabilities for respective γ -ray transitions were obtained for more than 30 γ -ray peaks from the ^{90}Zr compound nucleus. Of these, 5 γ rays are found to be particularly intense and will be important for the theoretical analyses to obtain the decay branching ratios, G^{CN}_γ . To validate the present surrogate approach, a benchmark measurement to obtain the known $^{90}\text{Zr}(n,\gamma)$ cross section using the $^{92}\text{Zr}(p,d\gamma)$ reaction is underway.

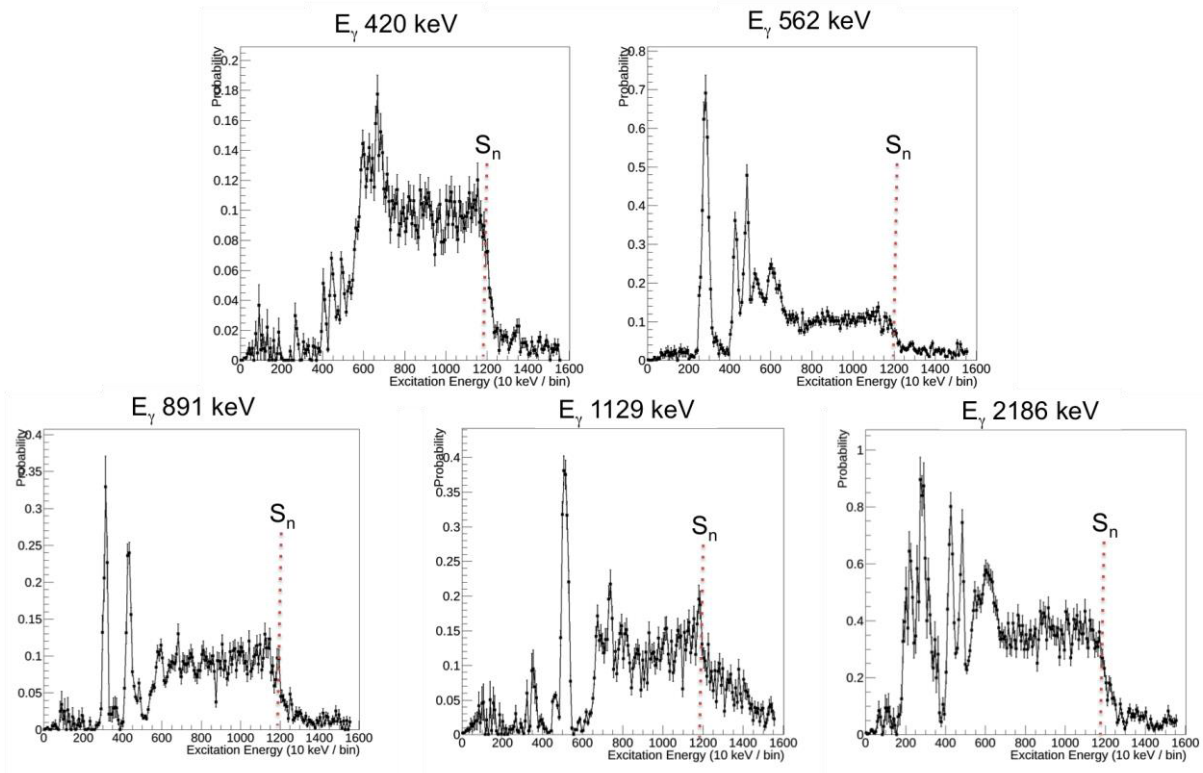


Figure 5. The probabilities ($P_{i(p,d\gamma)}$) for transitions of γ rays with energies of 420, 562, 891, 1129, and 2186 keV from ^{90}Zr .

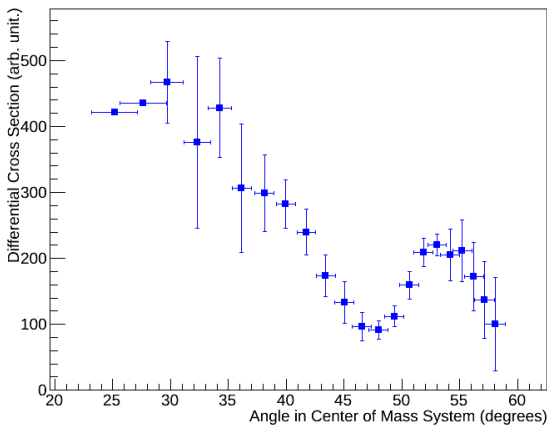


Figure 6. Deuteron angular distribution from the ^{90}Zr ground state (0^+).

Acknowledgements

We express our thanks to the cyclotron staff at Texas A&M University. This work was performed under the auspices of the US Department of Energy by Lawrence Livermore National Laboratory under contract No. DE-AC52-07NA27344. One of the authors, S. O. is supported by a JSPS Postdoctoral Fellowship for Research Abroad. Partial support through the US Department of Energy's Topical Collaboration TORUS is acknowledged.

References

1. D. Dean, J. Dobaczewski, K. Langanke, F. Nunes, and W. Ormand, RIA Theory Bluebook: A Road Map (RIA Theory Group) (2005)
2. T. Rauscher, P. Mohr, I. Dillmann, and R. Plag, APJ **738**, 143, (2011)
3. N. Colonna, Energy and Environmental Science **3**, 1910, (2010)
4. F.N. Mortensen, J.M. Scott, and S.A. Colgate, Los Alamos Sci. **28**, 38, (2003)
5. J. D. Cramer and H. C. Britt, Nucl. Sci. Eng. **41**, 177 (1970)
6. H. C. Britt and J. B. Wilhelmy, Nucl. Sci. Eng. **72**, 222 (1979)
7. J.E. Escher et al., Rev. Mod. Phys. **84**, 1 (2012)
8. J.E. Escher and F.S. Dietrich, Phys. Rev. C **74**, 054601 (2006)
9. J.D. Cramer and H.C. Britt, Phys. Rev. C **2**, 2350 (1970)
10. R. O. Hughes et al., Phys. Rev. C **85**, 024613 (2012)
11. G. Kessedjian et al., Phys. Lett. B **692**, 297 (2010)
12. J.J. Ressler et al., Phys. Rev. C **83**, 054610 (2011)
13. N.D. Scielzo et al., Phys. Rev. C **81**, 034608 (2010)
14. N.D. Scielzo et al., Phys. Rev. C **85**, 054619 (2012)
15. G. Boutoux et al. Phys. Lett. B **712**, 319 (2012)
16. J.E. Escher and F.S. Dietrich, Phys. Rev. C **81**, 024612 (2010)
17. C. Forssen et al., Phys. Rev. C **75**, 055807 (2007)
18. J.E. Escher, Conference Presentation at CNR*13 4th International Workshop on Compound-Nuclear Reactions and Related Topics, Maresias, Brazil (2013)
19. S.R. Leshner et al., Nucl. Instr. Meth. A **621**, 286 (2010)
20. J.B. Ball and C.B. Fulmer, Phys. Rev. **172**, 1199 (1968)

